MECSOL 2019 - Proceedings of the 7th International Symposium on Solid Mechanics
V. Tita, A. Ferreira, M.L. Ribeiro, A. Vieira and A.T. Beck (Editors), ABCM, Sao Carlos, SP, Brazil, April 15th to 17th, 2019

A Stress/Strain-Driven Homogenization Approach for the Uniaxial Analysis of Fibrous Soft Tissues

Mauricio Lazzari[1], Thiago André Carniel[1] and Eduardo Alberto Fancello[1,2]

[1] GRANTE - Department of Mechanical Engineering, Federal University of Santa Catarina, Florianópolis, SC, Brazil
[2] LEBm - University Hospital, Federal University of Santa Catarina, Florianópolis, SC, Brazil.

Abstract. The present manuscript provides a homogenization approach for the analysis of fibrous soft biological tissues. Since tensile tests are broadly applied to assess the mechanical responses of such materials, a proper multiscale boundary condition driven by strain and stress is proposed to account for the macroscopic constraints resulting from the macroscopic uniaxial stress condition. The proposed numerical strategy is consistently framed within a variational multiscale theory based on representative volume elements (RVE) and formulated at finite strains. A tensile test performed on a numerical specimen larger than the RVE is proposed as a reference solution. The numerical results point out that the present approach predicts with great accuracy not only the homogenized quantities but also the microscopic kinematic fields.
Keywords: multiscale, homogenization, finite element method, biological soft tissues

INTRODUCTION

Tensile tests are widely applied to assess the mechanical behavior of a broad range of fibrous soft tissues. Particularly for tendinous tissues - where the main physiological mechanical loadings occur in the axial direction of collagen fibers - uniaxial tensile tests comprise the main experimental approach to study their mechanical responses. In this case, the hypothesis of a homogeneous uniaxial stress state at the specimen scale (macroscopic scale) is generally assumed, i.e., the uniaxial stretch is known *a priori* and the transverse and shear components of the stress tensor are null. Based on this, one can verify that *one* kinematic constraint and *eight* stress conditions must be enforced to fulfill a uniaxial stress assumption.

On the other hand, multiscale theories based on representative volume elements (RVE) and formulated at finite strains generally comprise a *strain-driven* homogenization approach (Miehe et al., 2002; Blanco et al., 2014; de Souza Neto et al., 2015; Saeb et al., 2016). In other words, the deformation gradient at a macroscopic point must be known as the input data to the computational homogenization procedure and the macroscopic (homogenized) stress tensor is computed afterwards. Accordingly, one can note that a homogeneous macroscopic uniaxial stress state renders to a mixed multiscale approach driven by both stress and strain constraints.

Motivated by the aforementioned facts and aiming at multiscale numerical investigations of the mechanical behavior of tendon tissues, the present manuscript provides a computational homogenization approach for the analysis of fibrous soft materials submitted to uniaxial stress states. Based on this, a proper multiscale boundary condition mixing stress-driven and strain-driven approaches is proposed to account for the macroscopic kinematic and kinetic constraints resulting from the uniaxial assumption. The proposed numerical strategy is consistently framed within an RVE-based variational multiscale theory formulated at finite strains (de Souza Neto et al., 2015; Carniel et al., 2018). A tensile test performed on a numerical specimen larger than the RVE is proposed to verify the ability of the mixed boundary condition and related computational homogenization strategy to predict the multiscale responses. In this case, homogenized stress-stretch curves, macroscopic changes in volume and strains fields developed on the RVE are investigated.

METHODS

Computational homogenization at finite strains

The computational homogenization procedure employed in this work is derived from a finite strain RVE-based theory discussed by many authors (among others, Miehe et al. (2002), Blanco et al. (2014), de Souza Neto et al. (2015) and Saeb et al. (2016)). Following the incremental numerical approach described in Carniel et al. (2018), the current microscopic

displacements field $\mathbf{u}_{\mu_{n+1}}$ of the RVE is solution of the minimum principle

$$\left(\mathbf{u}_{\mu_{n+1}}\right)^{\text{opt}} = \arg \inf_{\mathbf{u}_{\mu_{n+1}} \in \mathcal{K}} \Psi, \qquad \Psi = \left\langle \mathcal{P}_\mu \right\rangle, \tag{1}$$

where $\Delta t = t_{n+1} - t_n$ is an increment of time, $\langle(\cdot)\rangle = \frac{1}{V_\mu}\int_{\Omega_{\mathbf{Y}}} (\cdot)\, \mathrm{d}V_\mu$ is the volumetric average of the quantity $(\cdot)$ and V_μ is the volume of the RVE in the referential (undeformed) domain $\Omega_{\mathbf{Y}}$ with boundaries $\Gamma_{\mathbf{Y}}$.

In Equation (1), Ψ is a macroscopic potential defined as the volumetric average of the microscopic incremental potential $\mathcal{P}_\mu$ used in variational constitutive approaches (see Ortiz and Stainier (1999) for further details on variational constitutive modeling). The space $\mathcal{K}$ in (1) represents multiscale boundary conditions that impose constraints on the microscopic displacements field. In this regard, the next section addresses a detailed discussion on the boundary condition studied in present manuscript. Once a solution is obtained from (1), the homogenization equation $\mathbf{P}_{n+1} = \left\langle \mathbf{P}_{\mu_{n+1}} \right\rangle$ establishes the micro to macro transition for the incremental first Piola-Kirchhoff stress tensor.

Proposed Multiscale Boundary Condition

Aiming at multiscale analyses of tendon tissues, the numerical investigation reported in Carniel et al. (2018) points out that the classical boundary conditions, namely, the linear boundary displacements model, the periodic boundary displacements model and the minimally constrained model, are not suitable choices for RVEs reinforced with helical fibers (similar to that shown in Figure 1c). Based on this, the aforementioned authors suggested a new boundary condition mixing characteristics of the linear and minimal models, called the *Mixed Axial-Linear Minimal Model* (MALM), which is defined as $\mathcal{K}^{\text{MALM}} \stackrel{\text{def}}{=} \left\{ \mathbf{u}_\mu \in \mathcal{K}^{\text{min}} \mid (\mathbf{u}_\mu)_1 = (\mathbf{u})_1 + [(\nabla_{\mathbf{X}}\mathbf{u})\,\mathbf{Y}]_1 ; \forall \mathbf{Y} \in \widehat{\Gamma} \right\}$, where $\mathcal{K}^{\text{min}} \stackrel{\text{def}}{=} \left\{ \mathbf{u}_\mu \mid \mathbf{F} - \langle \mathbf{F}_\mu \rangle = \mathbf{0};\ \mathbf{u} - \langle \mathbf{u}_\mu \rangle = \mathbf{0} \right\}$ is the minimally constrained model and $\mathbf{F}$, $\mathbf{F}_\mu$ are the macroscopic and microscopic deformation gradients, respectively. In the space $\mathcal{K}^{\text{MALM}}$, $\widehat{\Gamma} \stackrel{\text{def}}{=} \Gamma_{\text{front}} \cup \Gamma_{\text{back}}$ and Γ_{front}, Γ_{back} are the boundaries of the RVE oriented transversely to fibers (see Figure 1c). One can see from space $\mathcal{K}^{\text{MALM}}$ that only the axial contribution $(\mathbf{u}_\mu)_1$ of the linear boundary displacements model - which is oriented axially to fibers (aligned in the direction Y_1 of Figure 1c) - is imposed on boundaries Γ_{front} and Γ_{back} and the remaining degrees of freedom of the RVE are treated by the minimally constrained model $\mathcal{K}^{\text{min}}$.

At this point, it is important mentioning that the multiscale theory presented so far comprises a *strain-driven* homogenization approach, in the sense that the macroscopic deformation gradient $\mathbf{F}$ and the displacement $\mathbf{u}$ at a macroscopic point must be known as the input data to the homogenization procedure. However, a homogeneous macroscopic uniaxial stress state comprises a mixed approach driven by stress and strain. In other words, one kinematic constraint $(\mathbf{F})_{11} - \left\langle (\mathbf{F}_\mu)_{11} \right\rangle = 0$ (*strain-driven*) and eight stress conditions $(\mathbf{P})_{ab} = 0$, $a,b = 1\ldots3$, $ab \neq 11$ (*stress-driven*) are known *a priori*. Motivated by this fact, the space $\mathcal{K}^{\text{MALM}}$ is rewritten to properly account for the mentioned macroscopic uniaxial constraints, resulting in the space

$$\mathcal{K}^{\text{MALM}}_{\text{1D}} \stackrel{\text{def}}{=} \left\{ \mathbf{u}_\mu \in \mathcal{K}^{\text{min}}_{\text{1D}} \mid (\mathbf{u}_\mu)_1 = (\mathbf{u})_1 + [(\nabla_{\mathbf{X}}\mathbf{u})\,\mathbf{Y}]_1 ; \forall \mathbf{Y} \in \widehat{\Gamma} \right\}, \tag{2}$$

where $\mathcal{K}^{\text{min}}_{\text{1D}} \stackrel{\text{def}}{=} \left\{ \mathbf{u}_\mu \mid (\mathbf{F})_{11} - \left\langle (\mathbf{F}_\mu)_{11} \right\rangle = 0; \mathbf{u} - \langle \mathbf{u}_\mu \rangle = \mathbf{0};\ (\mathbf{P})_{ab} = 0; a,b = 1\ldots3, ab \neq 11 \right\}$ is the uniaxial counterpart of the the minimal model $\mathcal{K}^{\text{min}}$.

Numerical Solution

The proposed model $\mathcal{K}^{\text{MALM}}_{\text{1D}}$ is considered within the microscopic equilibrium through the following numerical strategy. Firstly, the constraints related to the space $\mathcal{K}^{\text{min}}_{\text{1D}}$ are enforced by the Lagrange multiplier method into the minimum principle (1), rendering to the unconstrained optimization problem

$$(\mathbf{x})^{\text{opt}} = \arg \operatorname*{stat}_{\mathbf{x}} \mathcal{L}(\mathbf{x}), \qquad \mathcal{L}(\mathbf{x}) \stackrel{\text{def}}{=} \Psi + \Lambda \left[(\mathbf{F})_{11} - \left\langle (\mathbf{F}_\mu)_{11} \right\rangle \right] - \boldsymbol{\gamma} \cdot \langle \mathbf{u}_\mu \rangle + \sum_{\substack{a,b=1 \\ ab \neq 11}}^{3} \chi_{ab} (\mathbf{P})_{ab}, \tag{3}$$

where $\mathcal{L}(\mathbf{x})$ is the lagrangian functional and $\mathbf{x} \stackrel{\text{def}}{=} \left\{ \mathbf{u}_\mu, \Lambda, \boldsymbol{\gamma}, \chi_{ab} \right\}$ is the set of unknown variables. The vector $\boldsymbol{\gamma}$ and the scalars Λ, χ_{ab} are the Lagrange multipliers. For the sake of clarity, the time-discrete notation $(\cdot)_{n+1}$ is not shown in the above variables and will be omitted henceforward. The variational principle (3) is formulated to be solved by the classical

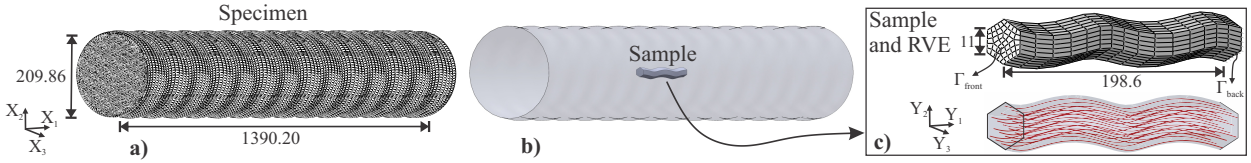

Figura 1 – (a) Finite element mesh and dimensions of the numerical specimen. (b) Sketch emphasizing the sample located in the centroid of the specimen. (c) Geometry, mesh and dimensions of the sample and of the RVE with two complete turns. Illustrative representation of the parallel distribution of the helical fibers within the mesh. Dimensions in micrometers.

Newton's procedure, where the nonlinear equations - obtained from the stationarity condition $\mathrm{d}\mathcal{L} = 0$ - are discretized by the standard finite element method. Finally, the prescribed displacements resulting from the linear boundary displacements model defined in $\mathcal{K}_{1\mathrm{D}}^{\mathrm{MALM}}$ are enforced in the degrees of freedom of the nodes belonging to the boundary $\widehat{\Gamma}$ into the linear system that computes the increments within the Newton-Raphson procedure (further technical details are addressed in Carniel et al. (2018)).

Verification Strategy

The verification of the proposed homogenization procedure follows the numerical strategy addressed in Carniel et al. (2018). In this case, a numerical test on a specimen sufficiently large in comparison to the size of the RVE is performed and the solution fields found at the inner part of the specimen are expected to be representative of what should be obtained on the RVE when submitted to appropriate homogenization procedures.

Following this approach, one considers the numerical *specimen* shown in Figure 1a-b, which is bioinspired by the microstructure of tendon fascicles and modeled with the transversely-isotropic constitutive model described in Carniel et al. (2018). In present case, helical fibers have crimp length of 99.3 μm and diameter of 4.6 μm (Kalson et al., 2015). Moreover, fibers are considered to be much stiffer than the matrix and they are distributed parallel to one another (see Figure 1c). The specimen contains two mesh regions. The external mesh presents a circular cross-section and it is designed to follow the helical geometry of fibers (see the helical wavy-like pattern shown in Figure 1a). The second mesh region consists on a small *sample* located on the centroid of this specimen (see Figure 1b).

The proposed RVE is a separate mesh conceived to follow the exact same geometry of the sample (Figure 1c). It is worth mentioning that the specimen, sample and RVE share identical meshes, and thus numerical results are comparable in a consistent manner.

The axial first Piola-Kirchhoff stress of the specimen is computed by the ratio between the resulting axial force f_{axial} and the undeformed cross section area of the specimen A, i.e., $(\mathbf{P})_{11} \overset{\mathrm{def}}{=} f_{\mathrm{axial}}/A$. The change in volume of the specimen is assessed by the volumetric jacobian, which is defined by the ratio between the current volume of the specimen v and the referential one V, i.e., $J \overset{\mathrm{def}}{=} v/V$. The corresponding macroscopic first Piola-Kirchhoff stress tensor and the volumetric jacobian obtained from the homogenization procedure are computed, respectively, by $\mathbf{P} = \langle \mathbf{P}_\mu \rangle$ and $J = \det(\mathbf{F})$.

RESULTS

In order to verify how the microscopic kinematics is affected by the proposed homogenization approach, Figure 2a displays the deformation patterns of the mesh and the von Mises measure of the logarithmic strain field $\varepsilon_{\mathrm{eq}}$ on the sample and the same fields on the RVE.

Macroscopic axial stress-stretch curves and volumetric jacobians calculated from the large simulation (specimen) and those predicted from the homogenization procedure (RVE) are plotted in Figure 2b and 2c, respectively.

DISCUSSION AND FINAL REMARKS

Based on the microscopic strain fields depicted in Figure 2a, one can see that the proposed multiscale approach (RVE) provides very good results in comparison to those obtained from the large simulation (sample) for all the evaluated macroscopic axial stretches.

In the same manner, one can verify, once again, that the proposed homogenization strategy predicts with great accuracy both the macroscopic axial stress-stretch curve (Figure 2b) and the volumetric jacobian (Figure 2c) obtained from the large simulation on the specimen.

Comparing Figures 2a and 2b, an important micro-to-macro relation is pointed out. Up to a global stretch $(\mathbf{F})_{11} = 1.01$,

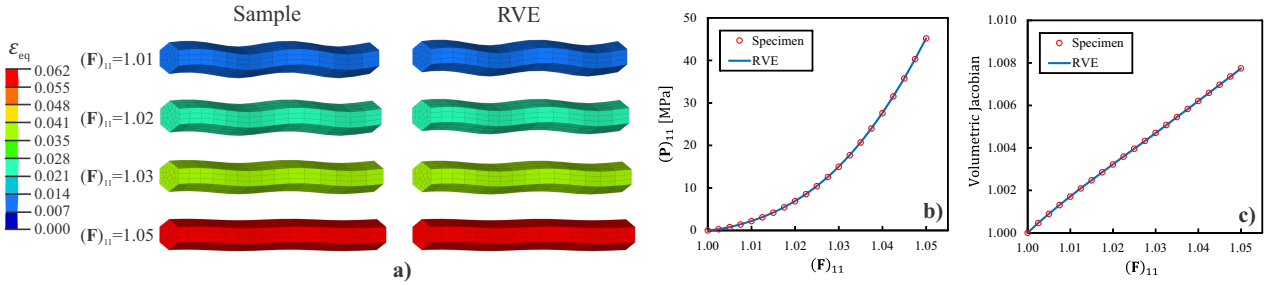

Figura 2 – (a) von Mises measure of the logarithmic strain on the sample and the same field on the RVE. Axial stress-stretch curves (b) and volumetric jacobians (c) computed from the specimen and those predicted from the proposed homogenization approach (RVE).

a low stiffness is verified, behavior that is mainly ruled by the matrix. Beyond $(\mathbf{F})_{11} = 1.01$, one can see that the stiffness increases due to the stretching of fibers. This particular behavior is usually observed in experimental tensile tests on tendon fascicles, since the RVE was bioinspired by this tissue. Moreover, this behavior reinforces the known concept that fibers rule the macroscopic axial stress-stretch response, since fibers are much stiffer structures than the surrounding matrices.

Another important issue concerns the homogenized volumetric jacobian plotted in Figure 2c. It is worth emphasizing that in the present homogenization approach, the macroscopic change in volume is a direct consequence of the microstructural response. In other words, a macroscopic axial stretch is imposed and the remaining components of the homogenized deformation gradient result from the homogenization procedure in order to respect the macroscopic stress constraints $(\mathbf{P})_{ab} = 0, a,b = 1\ldots3, ab \neq 11$ (see the space $\mathcal{K}^{\min}_{1\mathrm{D}}$ defined in (2)). This differs from a classical strain-driven multiscale approach where all components of $\mathbf{F}$, and consequently $J = \det(\mathbf{F})$, are input data. Accordingly, the multiscale numerical investigation of such mechanical conditions represents one of the main contributions of the present work.

Finally, the next step of this research aims to extend the present computational homogenization approach to study the multiscale responses of more complex RVEs of tendon fascicles. In this case, collagen fibers are treated as a new material phase within the RVE rather than structural components (fiber-reinforced model).

ACKNOWLEDGMENTS

The authors would like to thank the financial support provided by the Brazilian funding agencies CAPES - (Coordination for the Improvement of Higher Education Personnel) and CNPq - (National Council for Scientific and Technological Development).

REFERENCES

Blanco, P.J., Sanchez, P.J., de Souza Neto, E.A., Feijo, R.A., 2014. Variational Foundations and Generalized Unified Theory of RVE-Based Multiscale Models. Archives of Computational Methods in Engineering 23, 191–253.

Carniel, T.A., Klahr, B., Fancello, E.A., 2018. A multiscale numerical approach for the finite strains analysis of materials reinforced with helical fibers. Mechanics of Materials.

de Souza Neto, E., Blanco, P., Sánchez, P., Feijóo, R., 2015. An RVE-based multiscale theory of solids with micro-scale inertia and body force effects. Mechanics of Materials 80, 136–144.

Kalson, N.S., Lu, Y., Taylor, S.H., Starborg, T., Holmes, D.F., Kadler, K.E., 2015. A structure-based extracellular matrix expansion mechanism of fibrous tissue growth. eLife 4.

Miehe, C., Schotte, J., Lambrecht, M., 2002. Homogenization of inelastic solid materials at finite strains based on incremental minimization principles. Application to the texture analysis of polycrystals. Journal of the Mechanics and Physics of Solids 50, 2123–2167.

Ortiz, M., Stainier, L., 1999. The variational formulation of viscoplastic constitutive updates. Computer Methods in Applied Mechanics and Engineering 7825, 419–444.

Saeb, S., Steinmann, P., Javili, A., 2016. Aspects of Computational Homogenization at Finite Deformations: A Unifying Review From Reuss' to Voigt's Bound. Applied Mechanics Reviews 68.

RESPONSIBILITY NOTICE

The authors are the only responsible for the printed material included in this paper.